

## Sample Adaptive Offset Optimization in HEVC

\* Yang Zhang, Zhi Liu, Jianfeng Qu

North China University of Technology, Jinyuanzhuang Road 5th, Beijing, 100144, China

\* Tel.: +86 18801030451

\* E-mail: zyjohnyoung@126.com

*Received: 4 July 2014 /Accepted: 30 October 2014 /Published: 30 November 2014*

**Abstract:** As the next generation of video coding standard, High Efficiency Video Coding (HEVC) adopted many useful tools to improve coding efficiency. Sample Adaptive Offset (SAO), is a technique to reduce sample distortion by providing offsets to pixels in in-loop filter. In SAO, pixels in LCU are classified into several categories, then categories and offsets are given based on Rate-Distortion Optimization (RDO) of reconstructed pixels in a Largest Coding Unit (LCU). Pixels in a LCU are operated by the same SAO process, however, transform and inverse transform makes the distortion of pixels in Transform Unit (TU) edge larger than the distortion inside TU even after deblocking filtering (DF) and SAO. And the categories of SAO can also be refined, since it is not proper for many cases. This paper proposed a TU edge offset mode and a category refinement for SAO in HEVC. Experimental results shows that those two kinds of optimization gets -0.13 and -0.2 gain respectively compared with the SAO in HEVC. The proposed algorithm which using the two kinds of optimization gets -0.23 gain on BD-rate compared with the SAO in HEVC which is a 47 % increase with nearly no increase on coding time. *Copyright © 2014 IFSA Publishing, S. L.*

**Keywords:** High efficiency video coding (HEVC), Sample adaptive offset (SAO), Transform unit (TU).

### 1. Introduction

High Efficiency Video Coding (HEVC), which is under development by Joint Collaborative Team on Video Coding (JCT-VC), provides significant improvement on coding efficiency. HEVC aims to reduce bit rate in half with the same reconstructed video quality as H.264/advanced video coding, which is the latest-generation video coding [1, 2].

HEVC uses various transforms ranging from  $4 \times 4$  to  $32 \times 32$ , while AVC uses transforms no larger than  $8 \times 8$ . A larger transform could introduce more artifacts including ringing artifacts that mainly come from quantization errors of transform coefficients. Besides, HEVC uses 8-tap fractional luma sample interpolation and 4-tap fractional chroma sample interpolation, while AVC uses 6-tap and 2-tap for luma and chroma, respectively. A

higher number of interpolation taps can also lead to more serious ringing artifacts. So, HEVC adopted new in-loop filtering include deblocking filter (DF) and Sample Adaptive Offset (SAO). SAO, located after DF, is to reduce mean sample distortion of a region by three steps: classifying the region samples into multiple categories with a selected classifier, obtaining an offset for each category, and adding the offset to each sample of the category, where the classifier index and the offsets of the region are coded in the bitstream. Since SAO is a CTU (Coding Tree Unit)-based syntax design and DF is not an original-pixel based filter, there is no special consideration for the distortion in Transform Unit (TU) edge [3-7]. To reduce the distortion in TU edge, an improved SAO algorithm is proposed in this paper containing a TU edge mode Category Refinement for SAO is also proposed to improve the SAO performance.

This paper is organized as follows. Section 2 briefly describes the SAO process. Section 3 presents the proposed algorithm in this paper. Experimental results are shown in Section 4, and Section 5 concludes our study.

## 2. SAO Process in HEVC

The final design of HEVC has already adopted SAO in in-loop filtering. The key idea of SAO is to reduce sample distortion, it have been tested that SAO achieves 3.5 % BD-rate reduction on average with less than 1 % encoding time increase and about 2.5 % decoding time increase.

There are two types for SAO in HEVC: edge offset (EO) and band offset (BO).

### 2.1. Edge Offset

With the consideration of coding complexity and efficiency, as is shown in Fig. 1, EO used four patterns for sample classification: horizontal, vertical, 135° diagonal, and 45° diagonal. In Fig. 1, "c" represents the current pixel, "a" and "b" represent two neighboring pixel. For each CTU, the encoder selects one pattern from these four patterns, based on rate-distortion optimization.

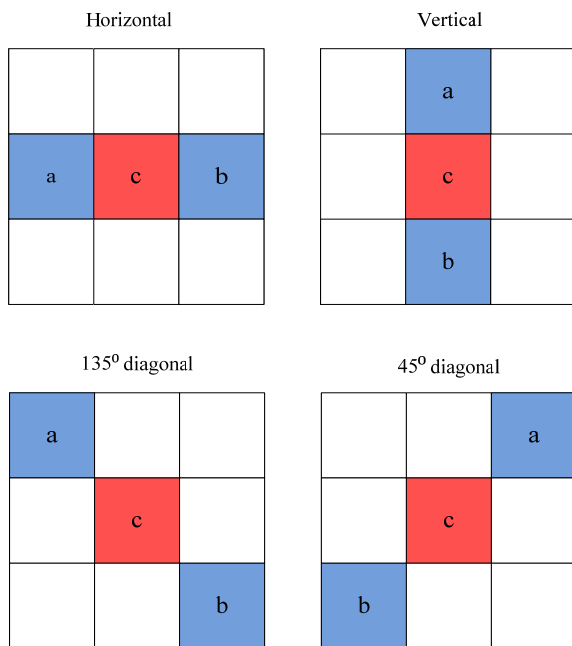


**Fig. 1.** Four 1-D directional patterns for EO sample classification: horizontal (EO class=0), vertical (EO class=1), 135° diagonal (EO class=2), and 45° diagonal (EO class=3).

To choose the best pattern, the encoder will full search every pattern. For a given EO class, each simple in a CTU is classified into one of the five categories, which is showed in Table 1 and Fig. 2. A

positive offset will be given for category 1 and category 2, while a negative offset will be given for category 3 and 4. Fig. 2 illustrates the meaning of edge offset signs. The meaning is to make the simple change smoother.

**Table 1.** Sample classification rules for edge offset.

Category	Condition
1	$c < a \ \&\& \ c < b$
2	$(c < a \ \&\& \ c == b) \    (c == a \ \&\& \ c < b)$
3	$(c > a \ \&\& \ c == b) \    (c == a \ \&\& \ c > b)$
4	$c > a \ \&\& \ c > b$
0	None of the above

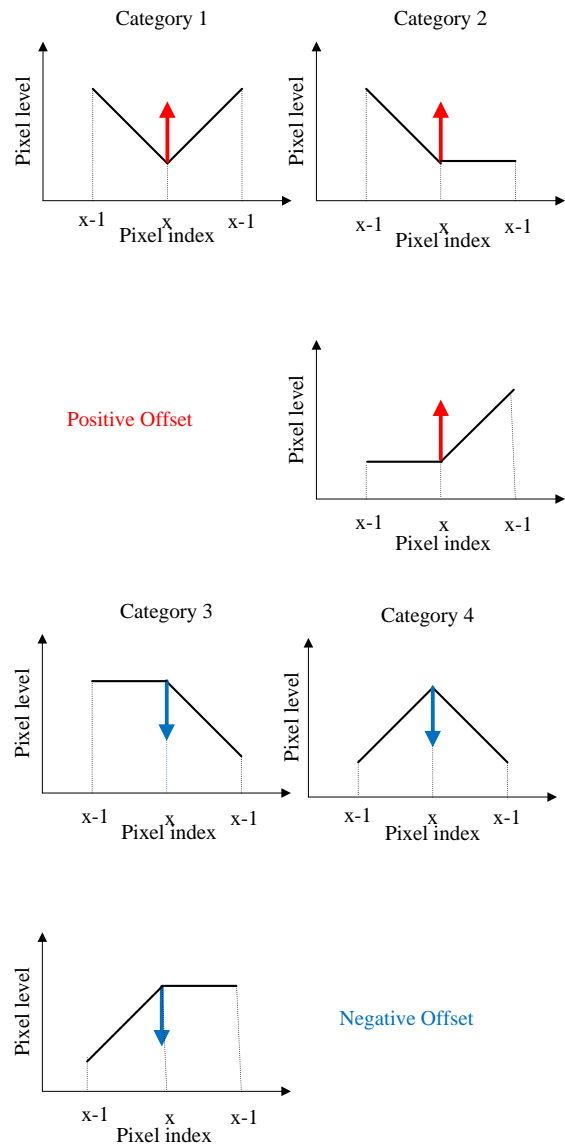


**Fig. 2.** Positive offsets for EO categories 1 and 2 and negative offsets for EO categories 3 and 4 result in smoothing.

After a simple is classified, the difference between original pixel value and reconstructed pixel value is calculated. The encoder, then, sums up the

difference and counts the number of all the sample with the same category in a CTU. The two values will be used to calculate the candidate offset in rate-distortion optimization.

## 2.2. Band Offset

Fig. 3 shows an example of sample distribution in a CTB when SAO using BO. In BO, the sample value, ranging from 0 to 255, is equally divided into 32 bands.

BO type means add one offset to the simple in the same band in a CTU.

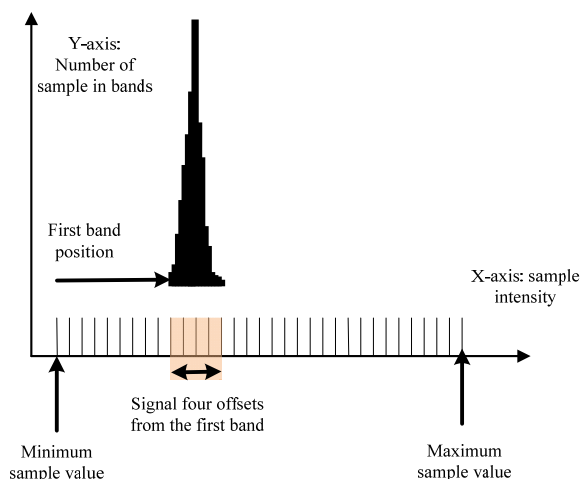


Fig. 3. Example of sample distribution in a CTB, where BO send the offsets of four consecutive bands.

The candidate offset is calculated under below:

$$h = \frac{\sum_{k \in C} (S_{org}(k) - S_{rec}(k))}{N}, \quad (1)$$

where  $h$  is the candidate offset,  $k$  is the sample position,  $C$  is the set of samples that are inside a CTB and belong to a specified SAO type (i.e., BO or EO), a specified starting band position or EO class, and a specified band or category.  $S_{org}$  is the original sample,  $S_{rec}$  represents the reconstructed sample.

## 3. The Proposed Algorithm

### 3.1. TU Edge Mode for SAO

As shown in Fig. 4, TU edge represent the pixels adjoin the TU boundary. TU edge usually introduce many artifacts after inverse transformation the quantized transform coefficients [8, 9].

Fig. 5 is an illustration shows the average distortion of a pixel inside TU and that of a pixel in TU edge in four different categories of EO. It can be observed that the distortion in TU edge is much

larger than the distortion inside TU even after in-loop filtering. In order to minimum the distortion in TU edge, this paper proposed an extra mode for SAO. The key point of this mode is give TU edge an extra offset, which may achieve lower distortion in TU edge and better RD performance.

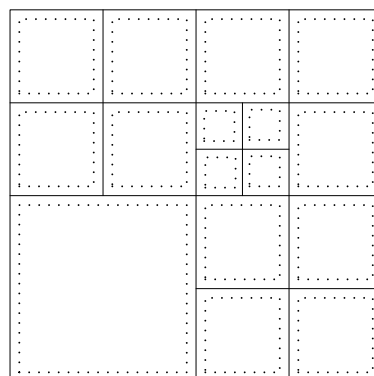
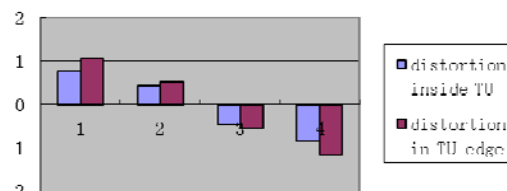
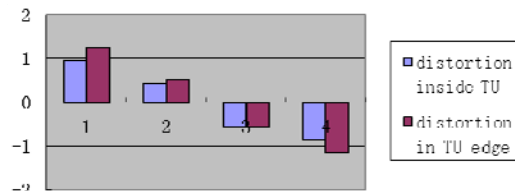


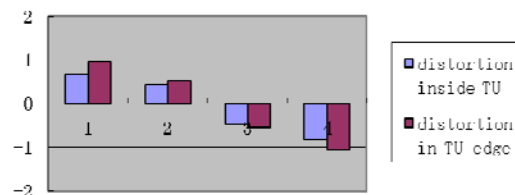
Fig. 4. TUs in a CU (Points present the pixels of TU edge).



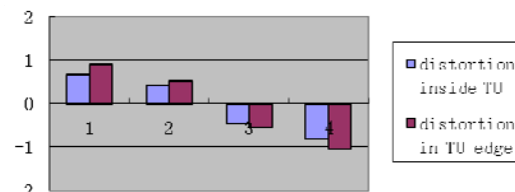
(a) EO class=0



(b) EO class=1



(c) EO class=2



(d) EO class=3

Fig. 5. Distortion inside TU and distortion in TU edge of the four categories in EO.

Fig. 5 shows that the distortion of TU edge got a 20 % larger on average than the distortion inside TU on average. To get the difference exactly, we count the offset value for TU edge and TU interior separately. The offset difference between TU edge and TU interior is shown in Table 2. From Table 2, we can see that the modulus of offset for TU edge gets 0.6 and 0.3, on average, larger than TU interior for EO category 1, 4 and category 2, 3. For BO type, which is not shown in Table 2, the offset difference is 0.4 on average.

Since the offset difference is very obvious for TU edge and interior, we designed several types for EO and BO. As is shown in Table 3, we actually designed 3 types for EO and BO, type 0 is the original type in SAO.

In the process of proposed mode, for a given EO or BO, the original offsets for TU edge and interior are calculate separately. After that, the offset with larger modulus will be passed into the RD process to choose the best offset for this CTU. The flowchart of TU edge mode is shown in Fig. 6.

**Table 2.** Offset difference in SAO.

Type Index	Offset difference on average			
	Category 2	Category 3	Category 1	Category 4
EO0	0.6	0.3	-0.3	0.6
EO1	0.6	0.3	-0.3	-0.6
EO2	0.5	0.3	-0.3	-0.6
EO3	0.6	0.3	-0.3	-0.6
Average	0.6	0.3	-0.3	-0.6

**Table 3.** Type index of TU edge mode SAO.

Type Index	Additional offset for TU edge in EO				Additional offset for TU edge in BO	
	Cat. 2	Cat. 3	Cat. 1	Cat. 4	Positive offset	Negative offset
0	0	0	0	0	0	0
1	0	0	1	-1	1	-1
2	1	-1	1	-1	2	-2
3	1	-1	2	-2	3	-3

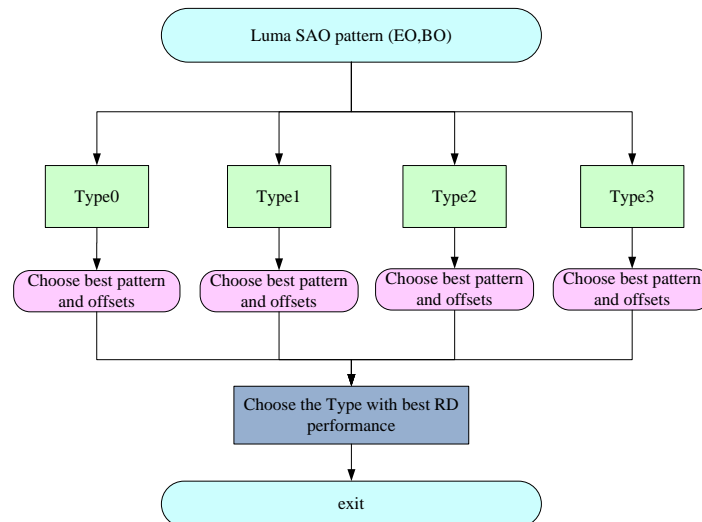


**Fig. 6.** Flowchart of the proposed algorithm.

### 3.2. Category Refinement for SAO

From section 2.1, Fig. 2 we can see that only when adjacent pixels are exactly the same, the current pixel can be judged to category 2, 3. In Fig. 7 we illustrate two kinds of unreasonable SAO category types. In Fig. 7 (a), category 2' and category 3' are two new categories which are not included in SAO. However these two categories are quite similar to category 2 and category 3, we tried to include the category 2' and category 3' into SAO. In Fig. 7(b), category 2'', 3'' are two special cases of category 2, 3, however the pixel of these two categories apparently do not additional offset. So we tried to remove these two special cases from SAO.

In the proposed algorithm these cases, which are shown in Fig. 8 (a), Fig. 8 (b), Fig. 8 (c) and Fig. 8 (d), are added into category 2 and 3, so that many

samples which need offsets are included in SAO. The two cases showed in Fig. 8 (e), Fig. 8 (f) are removed from SAO in the proposed algorithm.

### 3. Experimental Results

To evaluate the performance of the proposed algorithm, the up to 300 frames of each sequence were coded, and the test condition is "All Intra-Main" (AI-Main) [10]. QP values are set to 22, 27, 32, 37. A computer with a 2.8 GHz core was used in this experiment.

The anchor is the default HEVC encoder without SAO, and default HEVC encoder with SAO is also tested, whose results are also shown in Table 4 and Table 5.

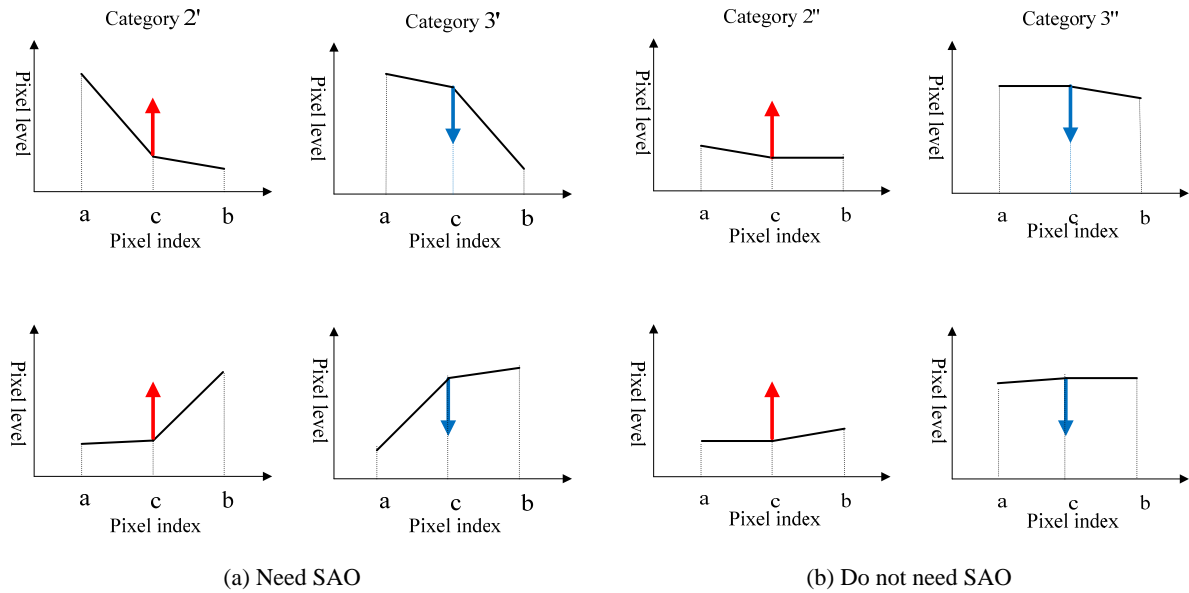


Fig. 7. Irrational categories.

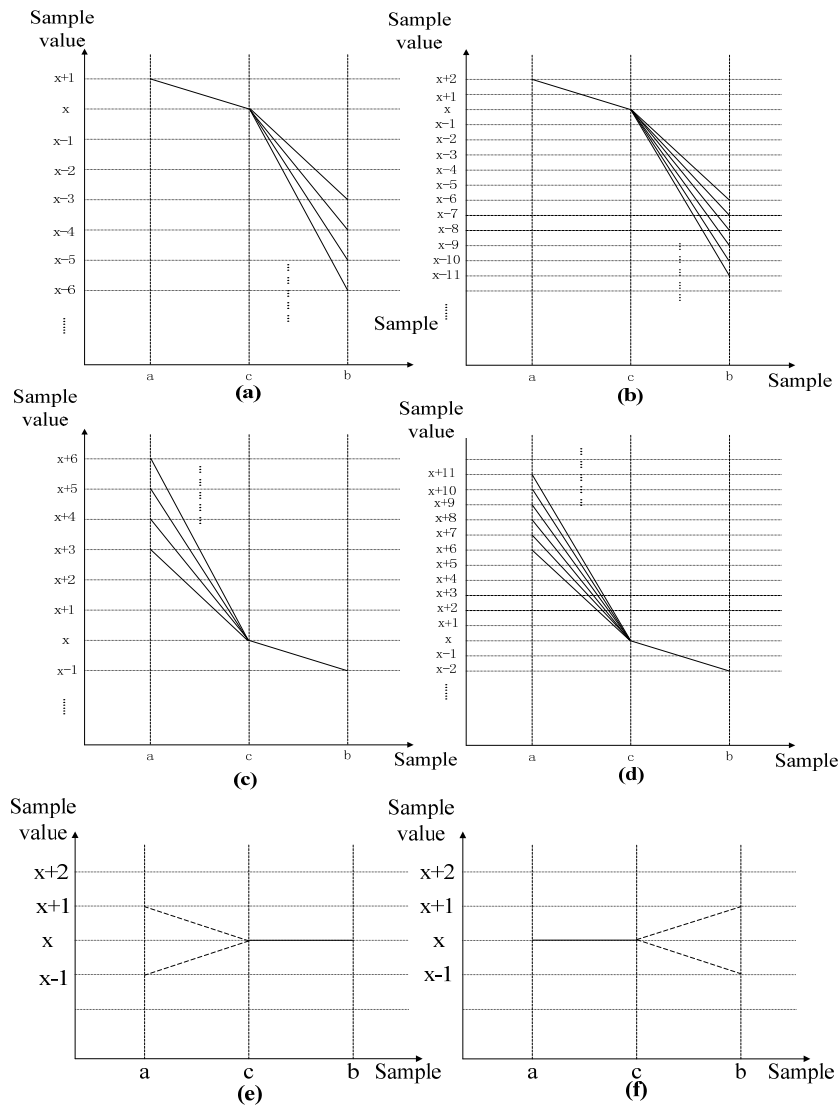


Fig. 8. Category refinement types.

**Table 4.** Results of TU edge mode SAO.

Sequence name		SAO BD-rate	TU edge mode SAO BD-rate	$\Delta$ BD-rate
Class B	Kimono	-0.5	-0.6	-0.1
	ParkScene	-0.7	-0.8	-0.1
	Cactus	-0.5	-0.6	-0.1
	BQTerrace	-0.5	-0.7	-0.2
Class C	BasketballDrill	-1.1	-1.1	0
	BQMall	-0.3	-0.6	-0.3
	PartyScene	-0.2	-0.3	-0.1
	RaceHorses	-0.6	-0.7	-0.1
Class D	BasketballPass	-0.3	-0.7	-0.4
	BQSquare	-0.5	-0.5	0
	BlowingBubbles	-0.2	-0.3	-0.1
	RaceHorses	-0.6	-0.7	-0.1
Average		-0.5	-0.63	-0.13

**Table 5.** Results of category refinement.

Sequence		SAO BD-rate	Category refinement BD-rate	$\Delta$ BD-rate
Class B	Kimono	-0.5	-0.7	-0.2
	ParkScene	-0.7	-0.8	-0.1
	Cactus	-0.5	-0.8	-0.3
	BQTerrace	-0.5	-0.7	-0.2
Class C	BasketballDrill	-1.1	-1.3	-0.2
	BQMall	-0.3	-0.5	-0.2
	PartyScene	-0.2	-0.3	-0.1
	RaceHorses	-0.6	-0.8	-0.2
Class D	BasketballPass	-0.3	-0.7	-0.4
	BQSquare	-0.5	-0.7	-0.2
	BlowingBubbles	-0.2	-0.3	-0.1
	RaceHorses	-0.6	-0.8	-0.2
Average		-0.5	-0.70	-0.20

From Table 4, we can see that the TU edge based SAO gets a -0.13 gain on BD-rate compare with the SAO in HEVC.

And from Table 5, we can see that after the category refinement, the BD-rate of HEVC got a -0.2 gain. The encoder time of the proposed algorithm, which is not listed, is almost the same as the anchor.

The improved SAO using both TU edge mode SAO and category refinement is more efficiency and the result is shown in Table 6, and the BD-rate of HEVC got a -0.23 gain.

#### 4. Conclusion

In this paper, we propose two kinds of SAO optimization for HEVC. From these experimental results we can see that, after our optimizations, the performance of SAO gets a 26 % and 40 % increase with negligible encoder time change. The improved SAO using both optimizations gets a 47 % increase compared with the SAO in HEVC. So our proposal on SAO optimization is valuable and is a topic worthy of further investigation.

**Table 6.** Results of TU edge mode SAO and category refinement.

Sequence		SAO BD-rate	Category refinement BD-rate	$\Delta$ BD-rate
Class B	Kimono	-0.5	-0.8	-0.3
	ParkScene	-0.7	-0.8	-0.1
	Cactus	-0.5	-0.8	-0.3
	BQTerrace	-0.5	-0.8	-0.3
Class C	BasketballDrill	-1.1	-1.3	-0.2
	BQMall	-0.3	-0.6	-0.3
	PartyScene	-0.2	-0.3	-0.1
	RaceHorses	-0.6	-0.8	-0.2
Class D	BasketballPass	-0.3	-0.8	-0.5
	BQSquare	-0.5	-0.7	-0.2
	BlowingBubbles	-0.2	-0.3	-0.1
	RaceHorses	-0.6	-0.8	-0.2
Average		-0.5	-0.73	-0.23

#### Acknowledgements

This work is supported by This work is supported by the Natural National Science Foundation of China (No. 61370111, No. 61103113), Beijing Municipal Education Commission General Program (KM201310009004) and Beijing Nova Program (Z14111000180000).

#### References

- [1]. G. J. Sullivan, J. R. Ohm, W. J. Han and T. Wiegand, Overview of the high efficiency video coding (HEVC) standard, *IEEE Transactions on Circuits and Systems for Video Technology*, Vol. 22, Issue 12, 2012, pp. 1649-1668.
- [2]. J. Nightingale, Q. Wang, C. Grecos, HEVStream: a framework for streaming and evaluation of high efficiency video coding (HEVC) content in loss-prone networks, *IEEE Transactions on Consumer Electronics*, Vol. 58, Issue 2, 2012, pp. 404-412.
- [3]. J. Zhu, D. Zhou, G. He, S. Goto, A combined SAO and de-blocking filter architecture for HEVC video decoder, in *Proceedings of the 20<sup>th</sup> IEEE International Conference on Image Processing (ICIP)*, Melbourne, VIC, 15-18 September 2013, pp. 1967-1971.
- [4]. P. N. Subramanya, R. Adireddy, D. Anand, SAO in CTU decoding loop for HEVC video decoder, in *Proceedings of the International Conference on Signal Processing and Communication (ICSC)*, Noida, 12-14 December 2013, pp. 507-511.
- [5]. G. B. Praveen and R. Adireddy, Analysis and approximation of SAO estimation for CTU-level HEVC encoder, in *Proceedings of the Conference on Visual Communications and Image Processing (VCIP)*, Kuching, 17-20 November 2013, pp. 1-5.
- [6]. W. Kim, Marta J. Sole, Offset Scaling in SAO for high bit-depth video coding, in *Proceedings of the 13<sup>th</sup> Conference on Joint Collaborative Team on Video Coding (JCT-VC) Meeting*, Incheon, KR, 18-26 April 2013, JCTVC-M0335.
- [7]. G. Laroche, T. Poirier, C. Gisquet, E. François, P. Onno, On inter-layer SAO for base mode, in *Proceedings of the 12<sup>th</sup> Conference on Joint*

Collaborative Team on Video Coding (JCT-VC) Meeting, Geneva, CH, 14-23 January 2013, JCTVC- L107.

- [8]. S. Ahn, M. Kim, Adaptive loop filtering based interview video coding in an hybrid video codec with MPEG-2 and HEVC for stereoscopic video coding, in *Proceedings of the 11<sup>th</sup> IEEE IVMSW Workshop*, Seoul, 10-12 June 2013, pp. 1-4.
- [9]. H. H. Bai, C. Zhu and Y. Zhao, Optimized multiple description lattice vector quantization for wavelet image coding, *IEEE Transactions on Circuits and Systems for Video Technology*, Vol. 17, Issue 7, 2007, pp. 912-917.
- [10]. F. Bossen, Common test conditions and software reference configurations, in *Proceedings of the 12<sup>th</sup> Conference on Joint Collaborative Team on Video Coding (JCT-VC) Meeting*, Geneva, CH, 14-23 January 2013, JCTVC-L1100.

---

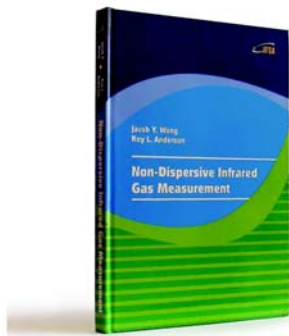
2014 Copyright ©, International Frequency Sensor Association (IFSA) Publishing, S. L. All rights reserved.  
(<http://www.sensorsportal.com>)



International Frequency Sensor Association (IFSA) Publishing

**Jacob Y. Wong, Roy L. Anderson**

## **Non-Dispersive Infrared Gas Measurement**



Formats: printable pdf (Acrobat) and print (hardcover), 120 pages

ISBN: 978-84-615-9732-1,  
e-ISBN: 978-84-615-9512-9

Written by experts in the field, the *Non-Dispersive Infrared Gas Measurement* begins with a brief survey of various gas measurement techniques and continues with fundamental aspects and cutting-edge progress in NDIR gas sensors in their historical development.

- It addresses various fields, including:
- Interactive and non-interactive gas sensors
- Non-dispersive infrared gas sensors' components
- Single- and Double beam designs
- Historical background and today's of NDIR gas measurements

Providing sufficient background information and details, the book *Non-Dispersive Infrared Gas Measurement* is an excellent resource for advanced level undergraduate and graduate students as well as researchers, instrumentation engineers, applied physicists, chemists, material scientists in gas, chemical, biological, and medical sensors to have a comprehensive understanding of the development of non-dispersive infrared gas sensors and the trends for the future investigation.

[http://sensorsportal.com/HTML/BOOKSTORE/NDIR\\_Gas\\_Measurement.htm](http://sensorsportal.com/HTML/BOOKSTORE/NDIR_Gas_Measurement.htm)